Dual-Band Bandpass Filter Incorporating Dual-Mode and Single-Mode Resonators

Shou-Jia Sun*, **Pan Yin, Yu-Ning Feng, and Xinshe Yin**

Abstract—This paper presents a novel dual-band bandpass filter by utilizing a new dual-mode resonator and a pair of single-mode split-ring resonators. The center frequencies and bandwidths of both passbands can be independently adjusted without affecting each other. Meanwhile, a capacitive source-load coupling is introduced to create transmission zeros near the passband edges, and the filter can obtain high skirt-selectivity. Such a dual-band bandpass filter operating at 3.5 GHz and 5.85 GHz with compact size is designed and fabricated.

1. INTRODUCTION

As a key component filtering unwanted signal in RF systems, dual-band BPFs have become more and more attractive in the application of wireless communication. To meet the demand, much research work and various design methods on dual-band BPFs have been presented [1–12]. Among them, the practice to cascade single-mode resonators, e.g., stepped-impedance resonators (SIRs), stub-loaded resonators (SLRs), and E-shaped resonators, is adopted for dual-band BPFs designs [1–6]. However, the resonant frequencies are dependent, and the size is too large for modern wireless systems. Recently, dual-mode resonators in filter applications have achieved great development. Dual-band BPFs can also be realized by adopting two dual-mode resonators with different sizes or one dual-mode resonator with the harmonic frequency operating at the second passband [7–12].

In this paper, we present a novel approach to design a dual-band BPF by incorporating a dual-mode resonator and single-mode split-ring resonators to generate dual-band response, and the dual-mode resonator is realized by a new proposed structure. In addition, the double feed lines are located between two types of resonators to eliminate mutual coupling. As a result, the center frequency and bandwidth for each passband can be freely adjusted. In order to improve the skirt-selectivity, source-load coupling is introduced to create transmission zeros near the passband edges. Based on the proposed design approach, a filter example is implemented. The comparison of measured and simulated results shows good agreement.

2. CHARACTERISTIC ANALYSIS OF FILTER

The proposed dual-band BPF structure is depicted in Fig. 1(a). A novel dual-mode resonator 1 and a pair of single-mode resonators 2 are employed to implement dual-band response. The former operates at the first passband, while the later is utilized to construct the second passband. In addition, source-load coupling exists in this structure through the small gap between the input and output feed lines. The topology of the proposed filter is shown in Fig. 1(b), in which the hollow and black nodes represent source/load and resonators, respectively. It can be observed from Fig. 1(a) that the dual-mode resonator 1 is symmetrical with respect to the plane T-T', so the odd-even-mode method is applied to analyze its resonant characteristics.
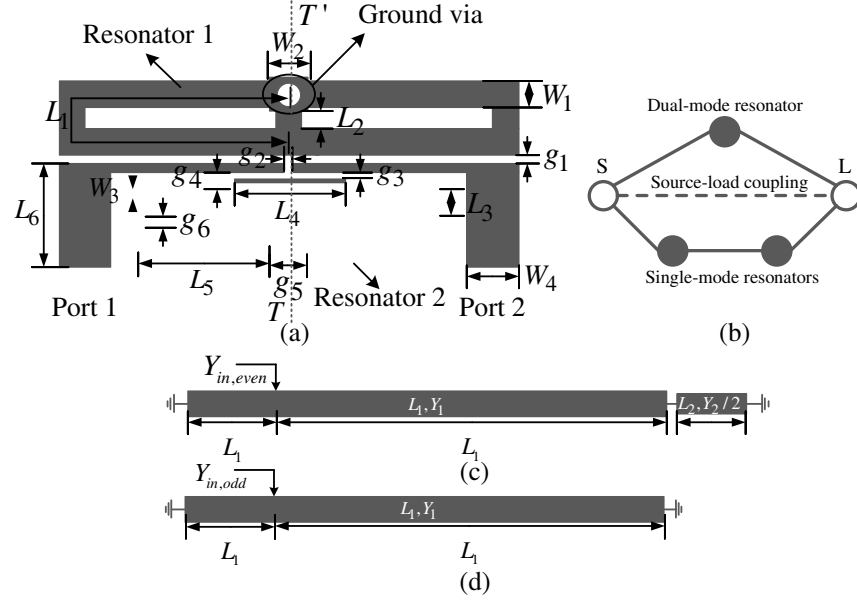
Figure 1. (a) Schematic and (b) topology of the proposed dual-band BPF. (c) Even- and (d) odd-mode equivalent circuit.

2.1. Analysis of the Proposed Dual-Mode Resonator 1

The even-mode equivalent circuit of the dual-mode resonator 1 is shown in Fig. 1(c), which can be achieved by adding a magnetic wall at the plane T-T'. Therefore, the stub with length L_2 is bisected, and its characteristic admittance is half what it was. The input admittance $Y_{in,even}$ concluded by the transmission theory is as

$$Y_{in,even} = -j\frac{Y_1}{\tan\theta_1'} - jY_1\frac{Y_2 - 2Y_1\tan\theta_1''\tan\theta_2}{2Y_1\tan\theta_2 + Y_2\tan\theta_1''} \tag{1}$$

where $\theta_i = \beta L_i$ represents the effective electrical length. According to the resonant condition $\text{Im}\{Y_{in,even}\} = 0$, there must be

$$Y_2\tan\theta_1 + 2Y_1\tan\theta_2 = 0 \tag{2}$$

For odd-mode excitation, its equivalent circuit is shown in Fig. 1(d), which can be modeled as an electric wall added along the symmetrical plane T-T'. With the stub ignored, the input admittance $Y_{in,odd}$ can be derived as

$$Y_{in,odd} = -j\frac{Y_1}{\tan\theta_1'} - j\frac{Y_1}{\tan\theta_1''} \tag{3}$$

By $\text{Im}\{Y_{in,odd}\} = 0$, we can obtain that

$$\tan\theta_1 = 0 \tag{4}$$

It can be seen from Eq. (4) that the odd-mode resonant frequency is only related to the length L_1 of the dual-mode resonator, and L_1 is equal to the half-wavelength. According to Eq. (2), when L_1 is fixed, the even-mode frequency varies with different lengths L_2 of the stub, while the odd-mode one remains constant. As shown in Fig. 2, when L_2 increases from 0.5 mm to 1.3 mm, the even-mode frequency decreases from 3.58 GHz to 3.4 GHz, and the odd-mode frequency operating at 3.95 GHz keeps unchanged. From the above analysis, the coupling strength in the dual-mode resonator can be adjusted by the length L_2 of the stub.

Because I/O feedlines are close to each other, source-load coupling comes into being. In order to enhance the coupling strength, an additional transmission line segment (hereinafter coupled line) with a length of L_4 is introduced. For demonstration, the simulation of the dual-mode resonator with weak
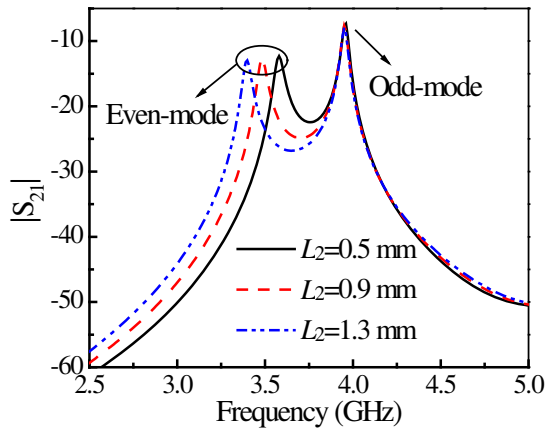
Figure 2. Simulated transmission response of the proposed dual-mode resonator under loose coupling with different L_2.
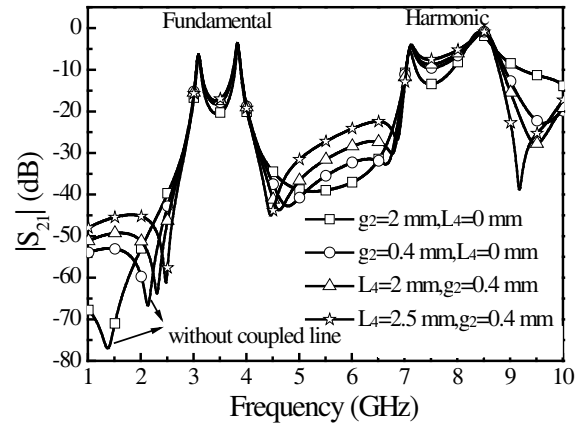
Figure 3. Simulated $|S_{21}|$ of the dual-mode resonator with and without source-load coupling.

external excitation is operated. As shown in Fig. 3, by increasing L_4 or decreasing g_2, source-load coupling gets stronger, and the transmission zeros move close to the fundamental passband, as well as the harmonic one, which leads to a higher skirt-selectivity.

The simulated results of the BPF realized by the dual-mode resonator are plotted in Fig. 4, which shows a high skirt-selectivity with two transmission zeros at 2.86 GHz and 4.8 GHz near the passband. Furthermore, the length of feed line approximately equals the quarter guide wavelength at the harmonic frequency, so a high harmonic suppression is obtained, with a wide stopband below −10 dB from 4.15 GHz to 11.07 GHz.

2.2. Design of the Proposed Dual-Band Filter

In order to obtain dual-band response, besides the dual-mode resonator operating at the first passband, a pair of single-mode split-ring resonators 2, as shown in Fig. 1(a), is adopted to form the second passband. Since the feed lines are located at the middle of two types of resonators, the mutual coupling is suppressed at maximum. As shown in Fig. 5, whatever resonators 2 are used or not, the response of the first passband is hardly affected. Vice versa, the dual-mode resonator 1 can be neglected when the single-mode resonators 2 are utilized to generate the second passband. In addition, a wide stopband below −10 dB from 6.17 GHz to 9.77 GHz is obtained in the dual-band response. Due to source-load coupling, transmission zeros are introduced, and the filter obtains high skirt-selectivity of both passbands.

3. FILTER DESIGN, FABRICATION AND MEASUREMENT

In this section, a dual-band BPF will be designed based on the above analysis, and the design specifications are listed in Table 1. According to filter synthesis in [13], the $[N + 2]$ ideal practical coupling matrixes of both passbands can be obtained as Eq. (5) for Band I and Eq. (6) for Band II.

Table 1. Design specifications of the proposed filter.

	f_0/GHz	BW/MHz	FBW	RL/dB
Band I	3.5	270	7.6%	18.5
Band II	5.85	240	4.1%	19.5
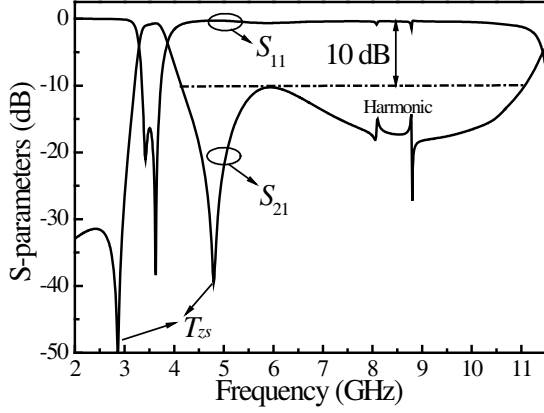
Figure 4. Simulated S-parameters of the dual-mode resonator.
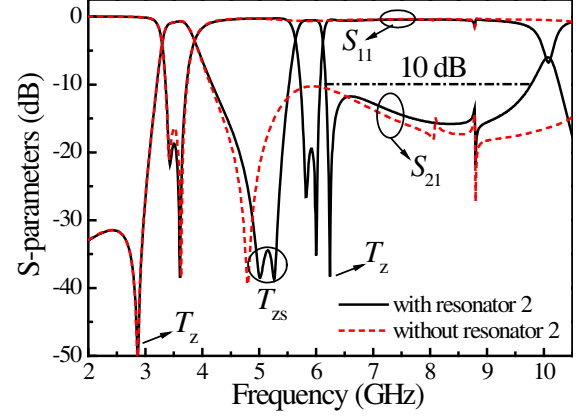
Figure 5. Simulated S-parameters of the proposed dual-band BPF with and without single-mode resonator 2.

$$[M]_1 = \begin{bmatrix} 0 & M_{So} & M_{Se} & M_{SL} \\ M_{So} & M_{oo} & 0 & M_{Lo} \\ M_{Se} & 0 & M_{ee} & M_{Le} \\ M_{SL} & M_{Lo} & M_{Le} & 0 \end{bmatrix} = \begin{bmatrix} 0 & -0.0347 & 0.0347 & 0.0036 \\ -0.0347 & -1.5499 & 0 & 0.0347 \\ 0.0347 & 0 & 1.5499 & 0.0347 \\ 0.0036 & 0.0286 & 0.0326 & 0 \end{bmatrix} \tag{5}$$

where the subscripts S, L, o and e represent source, load, odd- and even-modes in Resonator 1, respectively.

$$[M]_2 = \begin{bmatrix} 0 & M_{s1} & 0 & M_{SL} \\ M_{s1} & 0 & M_{12} & 0 \\ 0 & M_{12} & 0 & M_{2L} \\ M_{SL} & 0 & M_{2L} & 0 \end{bmatrix} = \begin{bmatrix} 0 & 0.0337 & 0 & 0.0036 \\ 0.0337 & 0 & 0.0637 & 0 \\ 0 & 0.0637 & 0 & 0.0337 \\ 0.0036 & 0 & 0.0337 & 0 \end{bmatrix} \tag{6}$$

where subscripts i $(i = 1, 2)$ represent two Resonators 2.

Based on the above analysis in Section 2.2, both passbands can be designed independently. Here, Band I is selected to be designed firstly. The odd- and even-mode frequencies can be calculated by the diagonal elements in the coupling matrix of Eq. (5), and the formula is

$$M_{ii} = \left(f_0^2 - f_i^2 \right) / \left(\Delta f \cdot f_i \right) \quad (i = o, e) \tag{7}$$

Here, parameters f_0 and Δf are the center frequency and bandwidth of Band I, respectively.

According to Eq. (7), the even- and odd-mode frequencies of Band I are 3.297 and 3.7155 GHz, respectively. The length $L_1 = 14.08$ mm can be obtained by substituting the odd-mode frequency into formula (4). Once length L_1 is fixed, tune length L_2 to achieve the even-mode frequency under weak coupling. Moreover, the external quality factors $Q = 16.6101$ of both modes can be calculated by the following formula

$$Q_i = \frac{1}{50 \times M_{si}^2} \quad (i = o, e) \tag{8}$$

As shown in Table 2, the external quality factors of both modes are directly proportional to parameter g_1, and $g_1 = 0.2$ mm is chosen to match in-band response.

And then, the length of resonator 2 can be determined easily, which is equal to half wavelength at the center frequency of Band II. Meanwhile, adjust g_4 and g_5 to satisfy the coupling coefficients in Eq. (6).

Finally, combining the dual-mode resonator 1 and a pair of resonators 2, make a minor tuning of g_1 and g_4 to obtain an optimum dual-band response.

Simulation is carried out using Zeland IE3D software, and the demonstration filter is designed on the substrate with a relative dielectric constant of 2.65 and thickness of 1 mm. The finally optimal geometric dimensions are given as $W_1 = 1$ mm, $W_2 = 1.6$ mm, $W_3 = 0.4$ mm, $W_4 = 2.7$ mm, $L_1 = 11.9$ mm,

Table 2. Extracted external quality factors under different parameter g_1.

g_1 (mm)	Q_{even}	Q_{odd}
0.1	13.3321	11.3029
0.15	15.1904	13.5618
0.2	17.2356	15.5815
0.25	19.4842	17.5624
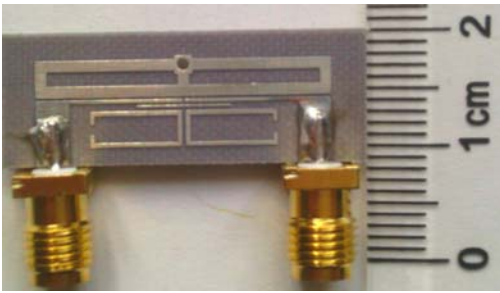
Figure 6. Photograph of the fabricated filter.
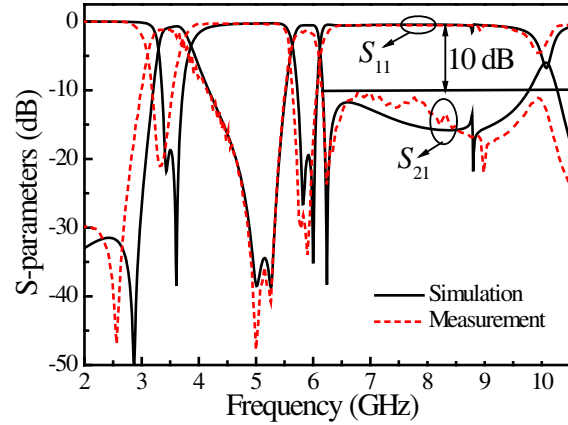
Figure 7. Simulated and measured S-parameters of the proposed dual-band BPF.

$L_2 = 3.2\,\text{mm}$, $L_3 = 1.1\,\text{mm}$, $L_4 = 7.9\,\text{mm}$, $L_5 = 8.2\,\text{mm}$, $L_6 = 5.8\,\text{mm}$, $g_1 = g_3 = 0.2\,\text{mm}$, $g_2 = 0.1\,\text{mm}$, $g_4 = 0.7\,\text{mm}$, $g_5 = 0.3\,\text{mm}$, $g_6 = 0.9\,\text{mm}$. Fig. 6 shows a photograph of the fabricated filter.

The measurement is implemented by Agilent's 8719ES network analyzer. Fig. 7 depicts the simulated and measured results. The first passband with fractional bandwidth of 8.8% works at 3.45 GHz, and the measured insertion loss is about 1.09 dB. The second passband with fractional bandwidth of 4.5% operates at 5.84 GHz, and the measured insertion loss is around 1.3 dB. Due to the source-load coupling, two transmission zeros, located at 5.0 GHz and 5.26 GHz between two passbands, are introduced to improve skirt-selectivity. Another two transmission zeros are located at 2.56 GHz and 6.24 GHz. In addition, a wide stopband below −10 dB from 6 GHz to 9.8 GHz is obtained in the dual-band response. The overall size of the filter is $0.31\lambda_g \times 0.13\lambda_g$, where λ_g is the guide wavelength of the first passband. Finally, Table 3 is provided to compare the proposed filter with those in [4, 5, 8, 12] in terms of a few key parameters. It is observed that the proposed filter in this paper occupies smaller size and lower insertion loss in passband.

Table 3. Performance comparison between the proposed filter and other techniques.

Ref.	Circuit Area ($\lambda_g \times \lambda_g$)	Insertion loss of center frequency (dB)	
		Band I	Band II
[4]	0.23×0.23	3.5	4.8
[5]	0.4×0.3	3	2.5
[8]	0.43×0.21	2.46	2.89
[12]	0.31×0.31	1.1	1.6
This work	0.31×0.13	1.09	1.3

4. CONCLUSION

In this paper, a new method to design dual-band BPF by incorporating dual-mode and single-mode resonators is presented. Since there is no mutual coupling between the two types of resonators, the center frequency and bandwidth can be independently designed for each passband. For a better skirt-selectivity property, the source-load coupling is introduced, and its coupling strength is enhanced by loading a coupled line. Moreover, this type of filter exhibits a good out-of-band rejection. At last, we summarize the design procedure for this type of filter. This method can be extended to other conditions such as combining dual-mode and triple- or quad-mode resonators. With flexible design freedoms and high performance, the proposed design method will be attractive to the design areas of dual-band and multi-band communication systems.

REFERENCES

1. Dai, G.-L., Y.-X. Guo, and M.-Y. Xia, "Dual-band bandpass filter using parallel short-ended feed structure," *IEEE Microw. Wireless Compon. Lett.*, Vol. 20, No. 6, 325–327, Jun. 2010.

2. Kuo, Y.-T. and C.-Y. Chang, "Analytical design of two-mode dual-band filters using E-shaped resonators," *IEEE Trans. Microw. Theory Tech.*, Vol. 60, No. 2, 250–260, Feb. 2012.

3. Wu, B., C.-H. Liang, Q. Li, and P.-Y. Qin, "Novel dual-band filter incorporating defected SIR and microstrip SIR," *IEEE Microw. Wireless Compon. Lett.*, Vol. 18, No. 6, 392–394, Jun. 2008.

4. Chen, J.-X., T. Y. Yum, J.-L. Li, and Q. Xue, "Dual-mode dual-band bandpass filter using stacked-loop structure," *IEEE Microw. Wireless Compon. Lett.*, Vol. 16, No. 9, 502–504, Sep. 2006.

5. Zhao, L.-P., D. Li, Z.-X. Chen, and C.-H. Liang, "Novel design of dual-mode dual-band bandpass filter with triangular resonators," *Progress In Electromagnetics Research*, Vol. 77, 417–424, 2007.

6. Wu, H.-W., Y.-F. Chen, and Y.-W. Chen, "Multi-layered dual-band bandpass filter using stub-loaded stepped-impedance and uniform-impedance resonators," *IEEE Microw. Wireless Compon. Lett.*, Vol. 22, No. 3, 114–116, Mar. 2012.

7. Sun, S.-J., T. Su, K. Deng, B. Wu, and C.-H. Liang, "Shorted-ended stepped-impedance dual-resonance resonators and its application to bandpass filters," *IEEE Trans. Microw. Theory Tech.*, Vol. 61, No. 9, 3209–3215, Sep. 2013.

8. Fu, S., B. Wu, J. Chen, S.-J. Sun, and C.-H. Liang, "Novel second-order dual-mode dual-band filters using capacitance loaded square loop resonator," *IEEE Trans. Microw. Theory Tech.*, Vol. 60, No. 3, 477–483, Mar. 2012.

9. Wang, J., L. G. Wang, and W. Wu, "Compact microstrip dual-mode dual-band bandpass filter with wide stopband," *Electron Lett.*, Vol. 47, No. 4, 263–265, Feb. 2011.

10. Li, Y. C., H. Wong, and Q. Xue, "Dual-mode dual-band bandpass filter based on a stub-loaded patch resonator," *IEEE Microw. Wireless Compon. Lett.*, Vol. 21, No. 10, 525–527, Oct. 2011.

11. Lee, J. and Y. Lim, "Compact dual-band bandpass filter with good frequency selectivity," *Electron Lett.*, Vol. 47, No. 25, 1376–1377, Dec. 2011.

12. Sung, Y., "Dual-mode dual-band filter with band notch structures," *IEEE Microw. Wireless Compon. Lett.*, Vol. 20, No. 2, 73–75, Feb. 2010.

13. Cameron, R. J., "Advanced coupling matrix synthesis techniques for microwave filters," *IEEE Trans. Microw. Theory Tech.*, Vol. 51, No. 1, 1–10, Jan. 2003.